CHAPTER 75

Bragg Reflection of Shallow-Water Waves on a Sloping Beach

Yong-Sik Cho[1] · Jong-In Lee[2] · Jong-Kyu Lee[3]

Abstract

In this study a set of governing equations describing the evolution of modulated shallow-water waves over a sinusoidally varying topography on a sloping beach is derived. The governing equations include the nonlinear interactions among different wave components as well as the shoaling effect over a slowly varying topography. It has been shown that the incident waves could be resonantly reflected by the interaction with the rippled seabed under the Bragg reflection condition. The magnitude of the resonantly reflected wave is almost equal to those of the incident and the transmitted waves.

1. Introduction

Water waves, approaching the coastline from deep water, undergo many physical phenomena caused by combined effects of bottom topographical variations, interference with man-made structures and nonlinear interactions among different wave components. One fascinating but challenging feature among these phenomena is so called the Bragg reflection occurring when the wave number of incident wave is a half of that of the sinusoidally varying topography. The Bragg reflection is believed to play an important role in the formation of submerged offshore sandbars frequently observed in Danish coast, the Great Lakes, Japanese coast and many other open coasts. In general, typical offshore multiple sandbars exist on beaches milder than 5 per 1000 and the number of sandbars varies 3 to 17 with a spacing of 10 m to 480 m between two adjacent bars (Mei and Liu, 1993).

[1]Assistant Professor, Dept. of Civil Engineering, Sejong University, Seoul, 143-747, KOREA
[2]Research Assistant, [3]Professor, Dept. of Civil Engineering, Hanyang University, Seoul, 133-791, KOREA

A lot of experimental and theoretical investigations have been performed to explain the possible formation mechanism of these sandbars as well as the effects of offshore sandbars on the change of the coastal morphology and the wave characteristics (Davies and Heathershaw, 1984; Mei, 1985; Yoon and Liu, 1987; Hara and Mei, 1987; Kirby and Vengayil, 1988; Liu and Cho, 1993). Through the laboratory experiment Carter et al. (1973) found that the formation of offshore sandbars is probably triggered by mass transport velocity near the seabed under partially reflected waves. They also pointed out that the incipient reflection coefficient for the sandbar formation is about 0.414. According to Mei and Liu (1993), a special bottom topography can reflect a significant amount of wave energy, and therefore can protect the beach from the possible erosion and deposit, that is, the strong reflection of incident waves could be the cause and the effect of offshore multiple sandbars.

Yoon and Liu (1987) investigated the near resonant reflection of periodic waves in shallow water over a sinusoidally varying topography. Since they were interested in near resonant reflection, only self-product terms of propagating wave components were considered. In this paper, we extend Yoon and Liu's study to examine the effects of the cross-product terms of oppositely propagating wave components and the number of seabed ripples. Thus, Yoon and Liu's study can be viewed as a limiting case of the present study. We also investigate the effect of a sloping beach on the reflection. Since the domain is fixed in shallow water, the Boussinesq equations are adequate to describe wave fields. The resonant reflection of incident periodic waves from a sinusoidally varying seabed laid on a sloping beach will be examined by solving a set of coupled nonlinear, ordinary differential equations. The effects of nonlinear interactions among different harmonics will also be examined for different numbers of seabed ripples.

In the following section, a set of governing equations describing modulation of shallow-water waves is first derived. These governing equations include effects of nonlinearity, dispersion, shoaling and interactions among different wave components. In section 3, two coupled ordinary differential equations are derived to describe evolution of water waves over a slowly varying topography. Numerical examples are given in section 4. Finally, concluding remarks are made in section 5.

2. Modulation Equations

By using a_0' as the characteristic wave amplitude, h_0' as the water depth and k' as the wave number, we introduce the following nondimensional variables:

$$(x, y) = k'(x', y'), \quad z = \frac{z'}{h_0'}, \quad h = \frac{h'}{h_0'},$$

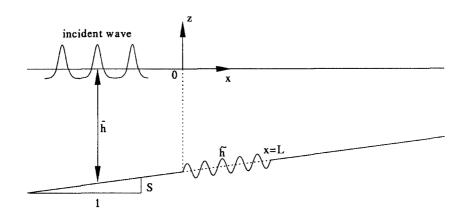$$t = k'\sqrt{gh_0'}\, t', \quad \zeta = \frac{\zeta'}{a_0'}, \quad u = \frac{h_0'}{a_0'(gh_0')^{1/2}}\, u'. \tag{1}$$

Figure 1. Definition sketch of the seabed and incident waves.

in which ζ' represents the free surface displacement and u' does the depth-averaged horizontal velocity vector. We also introduce following two parameters:

$$\varepsilon = \frac{a_0'}{h_0'}, \qquad \mu^2 = (k'h_0')^2 \tag{2}$$

in which ε and μ^2 represent the nonlinearity and the frequency dispersion, respectively. In the Boussinesq equations, orders of magnitude of both parameters are assumed to be equal and small enough. Using nondimensional variables the Boussinesq equations can be written in the following form (Yoon and Liu, 1987; Liu and Cho, 1993):

$$\frac{\partial \zeta}{\partial t} + \nabla \cdot [(h + \varepsilon \zeta) u] = 0, \tag{3}$$

$$\frac{\partial u}{\partial t} + \varepsilon u \cdot \nabla u + \nabla \zeta = \mu^2 \left\{ \frac{1}{2} h \frac{\partial}{\partial t} \nabla [\nabla \cdot (h u)] - \frac{1}{6} h^2 \frac{\partial}{\partial t} \nabla (\nabla \cdot u) \right\}. \tag{4}$$

It is noted that equation (3) is an exact expression, while equation (4) is truncated at the order of $O(\varepsilon^2, \varepsilon \mu^2, \mu^4)$.

To investigate resonant reflection and shoaling of incident waves over a slowly varying topography the water depth is defined as (see figure 1):

$$h(x, y) = \bar{h}(x, y) + \hat{h}(x, y) \tag{5}$$

in which

$$\bar{h}(x, y) \sim O(1), \qquad \hat{h}(x, y) \sim O(\mu^2) \tag{6}$$

and

$$|\nabla \bar{h}| \sim O(\mu^2), \qquad |\nabla \hat{h}| \sim O(\mu^2). \tag{7}$$

Following Yoon and Liu (1987) the free surface displacement and the velocity can be expressed in Fourier series. That is,

$$\zeta(x, y, t) = \frac{1}{2} \sum_n \zeta_n(x, y) \, e^{-int}, \tag{8}$$

$$\boldsymbol{u}(x, y, t) = \frac{1}{2} \sum_n \boldsymbol{U}_n(x, y) \, e^{-int} \tag{9}$$

in which a periodic motion in time has been assumed and $n = 0, \pm 1, \pm 2, \cdots$. In equations (8) and (9), ζ_{-n} and $\boldsymbol{U}_{-n}$ are the complex conjugates of ζ_n and $\boldsymbol{U}_n$, respectively. For simplicity, the symbols of $O(\varepsilon)$ and $O(\varepsilon^2)$ will be used to represent $O(\varepsilon, \mu^2)$ and $O(\varepsilon^2, \varepsilon\mu^2, \mu^4)$, respectively throughout the study.

By substituting equations (5)–(9) into equations (3) and (4), the following continuity and momentum equations are obtained for the nth Fourier components:

$$-in\zeta_n + \nabla \cdot (h \, \boldsymbol{U}_n) + \frac{1}{2}\varepsilon \sum_s \nabla \cdot (\zeta_s \, \boldsymbol{U}_{n-s}) = 0, \tag{10}$$

$$\begin{aligned}
-in \, \boldsymbol{U}_n + \frac{1}{2}\varepsilon \sum_s \boldsymbol{U}_s \cdot \nabla \, \boldsymbol{U}_{n-s} + \nabla \zeta_n \\
= -\frac{1}{3} in\mu^2 \, \bar{h}^2 \, \nabla(\nabla \cdot \boldsymbol{U}_n) = O(\varepsilon^2),
\end{aligned} \tag{11}$$

in which $s = 0, \pm 1, \pm 2, \cdots$. The leading order terms of equations (10) and (11) give

$$\zeta_n = -\frac{i}{n} \, \bar{h} \, \nabla \cdot \boldsymbol{U}_n + O(\varepsilon), \tag{12}$$

$$\boldsymbol{U}_n = -\frac{i}{n} \, \nabla \zeta_n + O(\varepsilon) \tag{13}$$

for $n \neq 0$ and

$$\boldsymbol{U}_0 = -\frac{\varepsilon}{2\bar{h}} \sum_s \zeta_s \boldsymbol{U}_{-s} + O(\varepsilon^2), \tag{14}$$

$$\zeta_0 = -\frac{1}{4}\varepsilon \sum_s \boldsymbol{U}_s \cdot \boldsymbol{U}_{-s} + O(\varepsilon^2) \tag{15}$$

for $n = 0$. Equations (14) and (15) represent steady components which have no contribution to other harmonics up to $O(\varepsilon)$. Thus, the steady components are excluded in this study. By eliminating the velocity vector from equations (10) and (11) and using equations (5), (12) and (13), we can obtain the following combined equation:

$$\begin{aligned}
n^2\zeta_n + \nabla \cdot (h \, \nabla \zeta_n) - \varepsilon \frac{\bar{h}}{2} \sum_{s \neq 0, n} \frac{1}{s(n-s)} \, \nabla \cdot [(\nabla \zeta_s \cdot \nabla) \nabla \zeta_{n-s}] \\
+ \frac{1}{3}\mu^2 \, \bar{h}^3 \, \nabla^4 \zeta_n + \varepsilon \frac{n}{2} \sum_{s \neq 0, n} \frac{1}{n-s} \, \nabla \cdot (\zeta_s \nabla \zeta_{n-s}) = O(\varepsilon^2).
\end{aligned} \tag{16}$$

The leading orders of equation (16) yield

$$\nabla^2 \zeta_n = -\frac{n^2}{\bar{h}} \zeta_n. \tag{17}$$

By substituting equation (17) into equation (16), we also obtain

$$\bar{h}\nabla^2\zeta_n + \nabla(\bar{h}+\hat{h})\cdot\nabla\zeta_n + n^2\left[1 - \frac{\hat{h}}{\bar{h}} - \frac{1}{3}\mu^2\bar{h}n^2\right]\zeta_n$$
$$= \varepsilon\sum_{s\neq0,n}\left\{\frac{\bar{h}}{2s(n-s)}\nabla\cdot[(\nabla\zeta_s\cdot\nabla)\nabla\zeta_{n-s}] - \frac{n}{2(n-s)}\nabla\cdot(\zeta_s\nabla\zeta_{n-s})\right\} \tag{18}$$

where $|\partial\zeta/\partial y|^2 \sim O(\varepsilon,\mu^2)$ has been assumed.

3. Evolution Equations

In this section we derive a set of coupled ordinary differential equations to describe evolution of waves over a slowly varying topography. After omitting y-direction components equation (18) can be rewritten as:

$$\bar{h}\frac{d^2\zeta_n}{dx^2} + \frac{d\bar{h}}{dx}\frac{d\zeta_n}{dx} + n^2\left(1 - \frac{\hat{h}}{\bar{h}} + \frac{1}{3}\mu^2\bar{h}n^2\right)\zeta_n$$
$$= \frac{\varepsilon}{2\bar{h}}\sum_{s\neq0,n}(n^2-s^2)\zeta_s\zeta_{n-s} - \frac{\varepsilon}{2}\sum_{s\neq0,n}\frac{n+s}{n-s}\frac{d\zeta_s}{dx}\frac{d\zeta_{n-s}}{dx} + O(\varepsilon^2). \tag{19}$$

The homogeneous leading order of equation (19) is the long wave equation and implies that wave components propagate both in $+x$ and $-x$ directions. Thus, the wave field can be split into the right- and the left-going components as (Liu and Cho, 1993):

$$\zeta_n = \zeta_n^+ + \zeta_n^- \tag{20}$$

where ζ_n^+ and ζ_n^- represent the right- and the left-going wave components, respectively. Then, the following coupled relationships can be obtained (Liu and Cho, 1993):

$$\frac{d\zeta_n^+}{dx} = \frac{in}{\bar{h}}\zeta_n^+ + F_n, \qquad \frac{d\zeta_n^-}{dx} = -\frac{in}{\bar{h}}\zeta_n^- - F_n \tag{21}$$

in which F_n is an unknown coupling term. By substituting equations (20) and (21) into equation (19) and after lengthy algebra, the coupling term F_n is determined as:

$$F_n = -\frac{1}{2\bar{h}}\left(\frac{1}{2}\frac{d\bar{h}}{dx} + \frac{d\hat{h}}{dx}\right)(\zeta_n^+ - \zeta_n^-) + \frac{in}{2\bar{h}}\left(-\frac{\hat{h}}{\bar{h}} + \frac{1}{3}\mu^2n^2\bar{h}\right)(\zeta_n^+ + \zeta_n^-)$$
$$-\frac{i\varepsilon}{4\bar{h}\bar{h}}\sum_{s\neq0,n}(n+s)\left[(\zeta_s^+\zeta_{n-s}^+ + \zeta_s^-\zeta_{n-s}^-) + \frac{n-2s}{n}(\zeta_s^-\zeta_{n-s}^+ + \zeta_s^+\zeta_{n-s}^-)\right]. \tag{22}$$

By assuming a periodic motion in space the wave components can be expressed as:

$$\zeta_n^+ = A_n(x)e^{in\Theta}, \qquad \zeta_n^- = B_n(x)e^{-in\Theta} \tag{23}$$

in which $A_n(x)$ and $B_n(x)$ are complex amplitude functions for the right- and the left-going waves, respectively and the following definition is used:

$$\Theta = \int\frac{dx}{\bar{h}}$$

Substituting equations (22) and (23) into equation (21), a set of coupled nonlinear ordinary differential equations can be obtained:

$$\frac{\mathrm{d}A_n}{\mathrm{d}x} + \left[\frac{in\hat{h}}{2\bar{h}\backslash\bar{h}} + \frac{1}{4}\frac{\mathrm{d}}{\mathrm{d}x}(\ln\bar{h}) + \frac{1}{2\bar{h}}\frac{\mathrm{d}\hat{h}}{\mathrm{d}x} - \frac{i}{6}\mu^2 n^3 \sqrt{\bar{h}} \right] A_n$$

$$- \left[-\frac{in\hat{h}}{2\bar{h}\backslash\bar{h}} + \frac{1}{4}\frac{\mathrm{d}}{\mathrm{d}x}(\ln\bar{h}) + \frac{1}{2\bar{h}}\frac{\mathrm{d}\hat{h}}{\mathrm{d}x} + \frac{i}{6}\mu^2 n^3 \sqrt{\bar{h}} \right] B_n \mathrm{e}^{-2in\Theta} \qquad (24\mathrm{a})$$

$$= \mathrm{NLT}_r + \mathrm{O}(\varepsilon^2)$$

where

$$\mathrm{NLT}_r = -\frac{i\varepsilon}{4\bar{h}\backslash\bar{h}} \sum_{s\neq 0,n} (n+s) \left[\left(A_s A_{n-s} + \frac{n-2s}{n} B_s A_{n-s} \mathrm{e}^{-2is\Theta} \right) \right]$$

$$- \frac{i\varepsilon}{4\bar{h}\backslash\bar{h}} \left[\sum_{s\neq 0,n} (n+s)(B_s B_{n-s} + \frac{n-2s}{n} A_s B_{n-s} \mathrm{e}^{2is\Theta}) \right] \mathrm{e}^{-2in\Theta}$$

for right-going waves,

$$\frac{\mathrm{d}B_n}{\mathrm{d}x} + \left[-\frac{in\hat{h}}{2\bar{h}\backslash\bar{h}} + \frac{1}{4}\frac{\mathrm{d}}{\mathrm{d}x}(\ln\bar{h}) + \frac{1}{2\bar{h}}\frac{\mathrm{d}\hat{h}}{\mathrm{d}x} + \frac{i}{6}\mu^2 n^3 \sqrt{\bar{h}} \right] B_n$$

$$- \left[\frac{in\hat{h}}{2\bar{h}\backslash\bar{h}} + \frac{1}{4}\frac{\mathrm{d}}{\mathrm{d}x}(\ln\bar{h}) + \frac{1}{2\bar{h}}\frac{\mathrm{d}\hat{h}}{\mathrm{d}x} - \frac{i}{6}\mu^2 n^3 \sqrt{\bar{h}} \right] A_n \mathrm{e}^{2in\Theta} \qquad (24\mathrm{b})$$

$$= \mathrm{NLT}_l + \mathrm{O}(\varepsilon^2)$$

where

$$\mathrm{NLT}_l = -\frac{i\varepsilon}{4\bar{h}\backslash\bar{h}} \sum_{s\neq 0,n} (n+s) \left[\left(B_s B_{n-s} + \frac{n-2s}{n} A_s B_{n-s} \mathrm{e}^{2is\Theta} \right) \right]$$

$$+ \frac{i\varepsilon}{4\bar{h}\backslash\bar{h}} \left[\sum_{s\neq 0,n} (n+s)(A_s A_{n-s} + \frac{n-2s}{n} B_s A_{n-s} \mathrm{e}^{-2is\Theta}) \right] \mathrm{e}^{2in\Theta}$$

for left-going waves. Equations (24a) and (24b) are evolution equations for waves propagating over a slowly varying topography.

In summary, equations (24a) and (24b) are the governing equations for shallow-water waves forced by self- and cross-product wave components. In equation (24) the terms multiplied by the exponential function and $\mathrm{d}\hat{h}/\mathrm{d}x$ are mathematically fast varying, whereas the other terms are slowly varying. The effects of the fast varying terms are generally insignificant, while they are significant if a phase is properly matched. Therefore, the present study is more general than Yoon ans Liu's (1987) in which all fast varying terms are ignored. The role of fast varying terms will be discussed in detail in the following section. After solving equation (24) the free surface profile of wave can be recovered as

$$\zeta(x,t) = \frac{1}{2}\sum_n [A_n \mathrm{e}^{in\Theta} + B_n \mathrm{e}^{-in\Theta}] \mathrm{e}^{-int}. \qquad (25)$$

The corresponding velocity up to the leading order can also be obtained by substituting equation (25) into equations (9) and (13).

4. Numerical Example

An iterative scheme is employed to solve coupled equations (24a) and

(24b) with prescribed initial conditions of A_n. In the iterative scheme the transmitted wave field is first solved without considering the reflected wave field. The reflected wave field is then estimated with the calculated transmitted wave. The transmitted wave field is finally updated with the newly obtained reflected wave field. The procedure is repeated until the converged solutions are obtained. More detailed description of the iterative scheme and the convergence condition are given in Liu and Cho (1993).

Now we examine the resonant reflection of incident periodic waves over a finite length of the rippled seabed. Although the shoaling effect is included in equation (25), we first focus on the Bragg reflection. Then, the shoaling effect over a sloping beach will also be examined later. In this study the nondimensional water depth is given as:

$$h = 1 - Sx, \qquad x \leq 0, \ x \geq L$$
$$h = 1 - Sx - \rho\sin(\delta x), \qquad 0 \leq x \leq L \tag{26}$$

in which ρ is the amplitude, S is the beach slope and δ is the wave number of the sinusoidally varying seabed. As mentioned in section 2, the orders of magnitudes of ρ and δ are $O(\mu^2)$ and $O(1)$, respectively. Figure 1 briefly illustrates the bottom topography consisting of sinusoidal ripples and a sloping beach as defined in equation (26).

In the first numerical example, we investigate the Bragg reflection of a train of cnoidal waves over a sinusoidally varying topography. Following Yoon and Liu (1987), the initial conditions for incident cnoidal waves are given as:

$$A_1 = 0.8923, \ A_2 = 0.4198, \ A_3 = 0.1568, \ A_4 = 0.0522, \ A_5 = 0.0163.$$

The number of harmonics is fixed at 5 throughout the study. Figure 2 shows the free surface profile of a train of cnoidal waves obtained by using 5 harmonics given above.
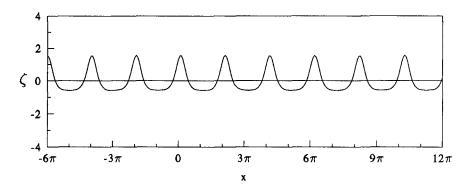

Figure 2. Free surface profile of the incident cnoidal waves at $t=0$.
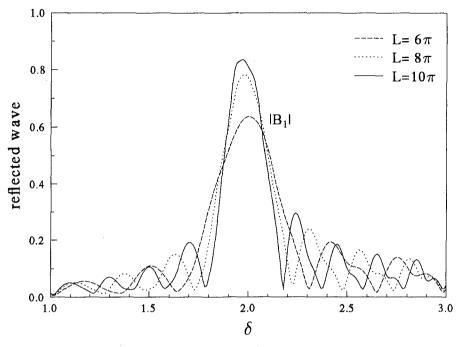
Figure 3. Reflected amplitude $|B_1|$ of cnoidal wave for
$n = 5$, $\varepsilon = 0.0881$, $\mu^2 = 0.1067$, $\rho = 0.15$.

To examine the effect of ripples on the reflection we calculate the reflected waves for three different numbers of ripples, that is, $m = 6$, 8 and 10 with m being the number of sinusoidal ripples. The reflection becomes stronger as the number of ripples increases as shown in figure 3. Therefore, the strongest reflection occurs when $m = 10$. We briefly explain the mathematics involved in the Bragg reflection. From equation (26)

$$\frac{dh}{dx} = \frac{d\tilde{h}}{dx} = -\rho\delta\cos(\delta x)$$
$$= -\rho\delta\frac{e^{i\delta x} + e^{-i\delta x}}{2} \tag{27}$$

By substituting equation (27) into equation (24b) the third term in the second parenthesis becomes

$$\frac{1}{2\bar{h}}\frac{d\tilde{h}}{dx}e^{2in\Theta}$$
$$= -\frac{\rho\delta}{4}[e^{i(\delta+2n)x} + e^{i(-\delta+2n)x}] \tag{28}$$

We can see that the second term of equation (28) becomes the unity if $\delta = 2n$. The second term of equation (28) varies slowly, whereas the first term does fast. Since the first harmonic dominates the incident wave system (Yoon and Liu, 1987), the forcing term of equation (24b) becomes largest

when $\delta = 2$, that is, the wave number of the ripple is twice that of the first harmonic of incident wave. As plotted in figure 3, the maximum reflection occurs at $\delta \approx 2$. The reflection coefficient is greater than 0.414 even for $m=6$.

The reflected waves for the first and the second harmonics are plotted with $L = 6\pi$ and $L = 10\pi$ in figures 4 and 5, respectively. The amplitude of the seabed ripple is fixed as $\rho = 0.1$ for both cases. The reflected waves without considering fast varying terms are slightly larger than those with considering fast varying terms. As stated previously, the magnitude of the first harmonic component is much larger than that of the second harmonic component. The difference between without considering and with considering fast varying terms is not surprising but appreciable. The beach slope is not considered both in figures 4 and 5.

In figure 6, the reflected waves for the first harmonic are plotted for $L = 10\pi$ and $\rho = 0.1$ with three different nonlinear effects. The strength of reflection is rapidly decreasing as the nonlinearity increases. This is because wave energy transfers more actively as the nonlinearity increases. That is, more wave energy transfers to higher harmonic components. The peak is also moving leftward as the nonlinearity increases.
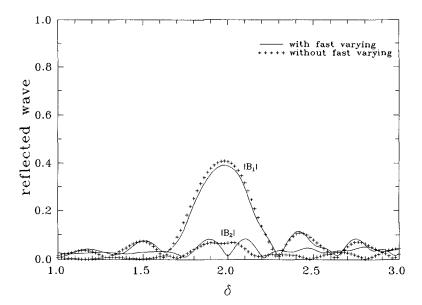

Figure 4. Reflected amplitudes of cnoidal wave for $L = 6\pi$, $S = 0.0$, $\varepsilon = 0.10$, $\mu^2 = 0.1067$, $\rho = 0.10$.
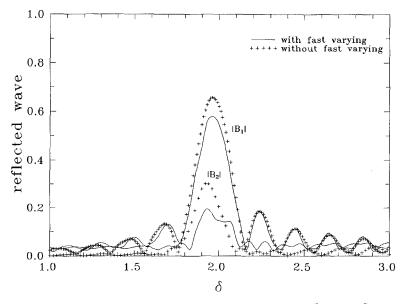
Figure 5. Reflected amplitudes of cnoidal wave for $L=10\,\pi$, $S=0.0$, $\varepsilon=0.10$, $\mu^2=0.1067$, $\rho=0.10$.
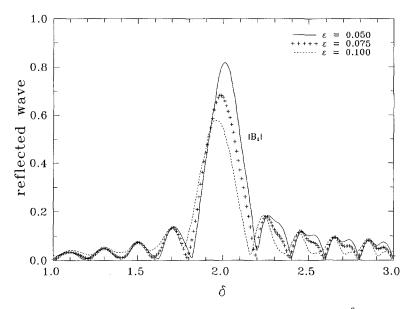

Figure 6. Effects of nonlinearity for $L=10\,\pi$, $S=0.0$, $\mu^2=0.1067$, $\rho=0.10$.

Finally, the first harmonic components of reflected waves are plotted in figures 7 and 8 for $L = 6\pi$ and $L = 10\pi$ with two different beach slopes, $S = 0$ and $S = 0.005$. The amplitude of the seabed ripple is also fixed as $\rho = 0.1$. The magnitudes of reflected waves remain almost the same in figures 7 and 8, respectively. This is because the beach slope $S = 0.005$ is too mild to affect to the magnitude of the reflected wave. As discussed in section 2, the order of magnitude of a beach slope is assumed to be $O(\mu^2)$ in this study. However, the slope used in figures 7 and 8 is 0.005 much smaller than $O(\mu^2)$. The peak moves slightly leftward as the beach slope increases.

5. Concluding Remarks

In this study a set of governing equations is derived from the Boussinesq equations to examine the evolution of periodic waves over a sinusoidally varying topography laid on a sloping beach. The derived governing equations are used to study the evolution of cnoidal waves over a slowly varying topography. It has been shown that reflected waves can be resonantly amplified under the Bragg reflection condition..
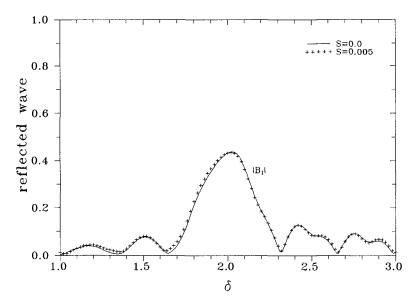
Figure 7. Comparison of reflected amplitudes for $L = 6\,\pi$, $\varepsilon = 0.075$, $\mu^2 = 0.10$, $\rho = 0.10$.
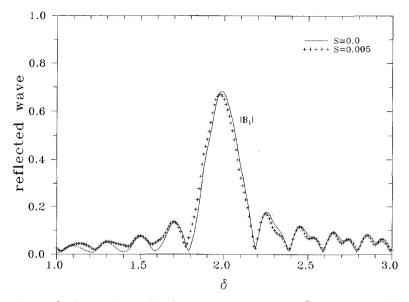
Figure 8. Comparison of reflected amplitudes for $L=10\,\pi$, $\varepsilon=0.075$, $\mu^2=0.10$, $\rho=0.10$.

In very shallow water the nonlinear effect may dominate the entire wave system. Especially, just before the breaking point waves might be highly nonlinear. Futhermore, the bottom friction becomes increasingly important as the water depth decreases. An extension with inclusion of highly nonlinear terms and the bottom friction is now progressing. The result will be reported in future.

Acknowledgment

References

Carter, T.G., Liu, P.L.-F., and Mei, C.C.(1973). "Mass transport by waves and offshore sand bedforms." J. Waterway, Port, Coastal and Ocean Eng., ASCE, Vol. 99, pp. 165-184.

Davies, A.G. and Heathershaw, A.D.(1984). "Surface wave propagation over sinusoidally varying topography." J. Fluid Mech., Vol. 144, pp. 419-443.

Hara, T. and Mei. C.C.(1987). "Bragg reflection of surface waves by periodic bars: Theory and experiment." J. Fluid Mech., Vol. 178, pp. 221-241.

Kirby, J.T and Vengayil, P.(1988). "Nonresonant and resonant reflection of long waves in varying channels." J. Geophys. Res., Vol. 93, pp. 10,782-10,796.

Liu, P.L.-F. and Cho, Y.-S.(1993). "Bragg reflection of infragravity waves by sandbars." J. Geophys. Res., Vol. 98, pp. 22,733-22,741.

Mei, C.C.(1985). "Resonant reflection of surface water waves by periodic bars." J. Fluid Mech., Vol. 152, pp. 315-335.

Mei, C.C. and Liu, P.L.-F.(1993). "Surface waves and coastal dynamics." *Annu. Rev. Fluid Mech.*, Vol. 25, pp. 215-240.

Yoon, S.B. and Liu, P.L.-F.(1987). "Resonant reflection of shallow-water waves due to corrugated boundaries." J. Fluid Mech., Vol. 180, pp. 451-469.